Magnetic Resonance Imaging 51 (2018) 151–157

Contents lists available at ScienceDirect

Magnetic Resonance Imaging

journal homepage: www.elsevier.com/locate/mri

Original contribution

Effects of global signal regression and subtraction methods on resting-state functional connectivity using arterial spin labeling data

João Paulo Santos Silva[1], Luciana da Mata Mônaco[1], André Monteiro Paschoal[1], Ícaro Agenor Ferreira de Oliveira[1], Renata Ferranti Leoni[*,1]

Inbrain Lab, Department of Physics, FFCLRP, University of Sao Paulo, Ribeirao Preto, Brazil

ARTICLE INFO

Keywords:
Functional arterial spin labeling
Artifact removal
Pairwise subtraction
Functional connectivity
Cerebral blood flow

ABSTRACT

Background: Arterial spin labeling (ASL) is an established magnetic resonance imaging (MRI) technique that is finding broader applications in functional studies of the healthy and diseased brain. To promote improvement in cerebral blood flow (CBF) signal specificity, many algorithms and imaging procedures, such as subtraction methods, were proposed to eliminate or, at least, minimize noise sources. Therefore, this study addressed the main considerations of how CBF functional connectivity (FC) is changed, regarding resting brain network (RBN) identification and correlations between regions of interest (ROI), by different subtraction methods and removal of residual motion artifacts and global signal fluctuations (RMAGSF).

Methods: Twenty young healthy participants (13 M/7F, mean age = 25 ± 3 years) underwent an MRI protocol with a pseudo-continuous ASL (pCASL) sequence. Perfusion-based images were obtained using simple, sinc and running subtraction. RMAGSF removal was applied to all CBF time series. Independent Component Analysis (ICA) was used for RBN identification, while Pearson' correlation was performed for ROI-based FC analysis.

Results: Temporal signal-to-noise ratio (tSNR) was higher in CBF maps obtained by sinc subtraction, although RMAGSF removal had a significant effect on maps obtained with simple and running subtractions. Neither the subtraction method nor the RMAGSF removal directly affected the identification of RBNs. However, the number of correlated and anti-correlated voxels varied for different subtraction and filtering methods. In an ROI-to-ROI level, changes were prominent in FC values and their statistical significance.

Conclusions: Our study showed that both RMAGSF filtering and subtraction method might influence resting-state FC results, especially in an ROI level, consequently affecting FC analysis and its interpretation. Taking our results and the whole discussion together, we understand that for an exploratory assessment of the brain, one could avoid removing RMAGSF to not bias FC measures, but could use sinc subtraction to minimize low-frequency contamination. However, CBF signal specificity and frequency range for filtering purposes still need to be assessed in future studies.

1. Introduction

Arterial spin labeling (ASL) is a noninvasive magnetic resonance imaging (MRI) technique for cerebral blood flow (CBF) quantification that has been recently used to investigate resting-state brain networks (RBNs) [1–3]. The specificity of ASL signal intrinsically related to cerebral metabolism and then neuronal activity turns the technique very interesting to obtain CBF time-series, allowing the assessment of an isolated hemodynamic parameter with a relatively simple experimental design [1,4,5]. However, because of low signal-to-noise ratio (SNR), spatial and temporal resolutions of ASL images, studying functional connectivity with CBF fluctuations is still at development regarding image acquisition and processing [3,6–11].

In ASL, the amount of signal related to blood perfusion is assumed to be proportional to the difference between control and label images. Then, CBF maps are calculated using the perfusion images and mathematical approaches [12,13]. However, different methods of subtraction have been used. The first one, simple subtraction, calculates the signal difference between one control-label pair to obtain one perfusion-based image. Although simple and widely used, it does not filter physiological noise [5,14]. Therefore, other methods have been proposed: (1) surround subtraction, which uses a mean control (or label) image averaged from two images acquired just before and after the label (or control) image, attenuating high frequency noise, such as the

* Corresponding author at: Department of Physics, FFCLRP, University of Sao Paulo, Av. Bandeirantes, 3900, 14040-901 Ribeirao Preto, Sao Paulo, Brazil.
E-mail address: leonirf@usp.br (R.F. Leoni).
[1] All authors equally contributed.

https://doi.org/10.1016/j.mri.2018.05.006
Received 28 March 2018; Received in revised form 4 May 2018; Accepted 14 May 2018

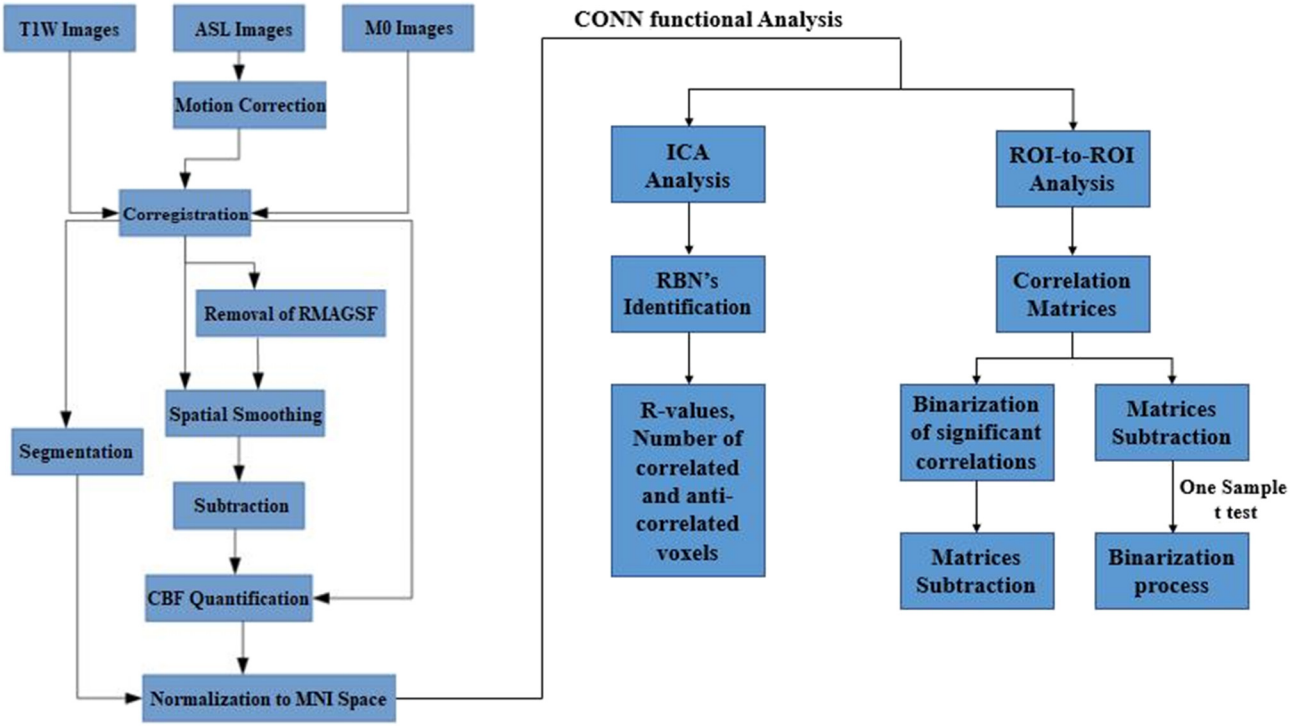

Fig. 1. Pipeline and analyzing image processing. RMAGSF: residual motion artifacts and global signal fluctuations.

cardiac one [5,14,15]; (2) sinc subtraction that consists of a temporal shifting correction for the delay time between control and label image acquisitions, acting like a band-pass filter [14–17]; and (3) running subtraction that increases the number of time points in CBF time series and improves temporal SNR [14,16].

Moreover, ASL images are affected by the blood oxygenation level dependent (BOLD) contamination. It is known that ASL images acquired with fast readouts, such as echo planar imaging (EPI), undergo a signal attenuation due to T2* effects [16,17], which are comparable to those observed in BOLD images and reflects other physiological parameters than CBF. This BOLD contamination is minimized when images are acquired with a reduced echo time (TE) [11]; however, reducing TE is limited due to consequent reduction of signal intensity [10,18]. Therefore, besides choosing an optimal TE (generally 8–15 ms), one may use a temporal filter to reduce signal with frequencies at the noise range (up to 0.02 Hz) or obtain perfusion-based images using a specific method of subtraction with sinc interpolation that acts like temporal filtering [14,19].

When analyzing brain functional connectivity, another issue to deal with is the baseline global signal inherent to the image acquisition and subject physiology, such as thermal noise [20]. Considered a noise that supposedly perturbs the fluctuations of interest, the global signal is generally removed in a preprocessing step, improving temporal SNR and test-retest reliability of CBF time series [20–22]. On the other hand, studies have reported that global signal is strongly coupled to low-frequency fluctuations and therefore it may be associated with the synchronism of all neurons, independently of their specific functions [23–25]. Therefore, it may contribute to the study of the brain at rest instead of being noise. So far, there is still no consensus about removing or not the global signal during image preprocessing.

Therefore, in the present study, we aimed to assess the effect of different methods of subtraction and the impact of residual motion artifact and global signal removal on the identification of RBNs and evaluation of functional connectivity using CBF time series of healthy young volunteers.

2. Methods

2.1. Subjects

Twenty healthy subjects (13 M/7F, [mean ± SD] = 25 ± 3 years old) participated in this study after reading and signing an informed consent approved by the Ethics in Research Committee of the Clinical Hospital, School of Medicine of Ribeirao Preto (HCFMRP). Exclusion criteria included the presence of pacemaker or prosthesis incompatible with the magnetic resonance environment; claustrophobia; dementia or cognitive impairment; diabetes, hypertension and neurological diseases; pregnancy; and not signing the consent form.

2.2. Image acquisition

Images were acquired on a 3T MRI system (Philips Achieva, The Netherlands) at the HCFMRP, using a 32-channel head coil for reception and a body coil for transmission. Resting-state pseudo-continuous ASL images were acquired using a 2D single-shot EPI sequence (TR/TE = 4000/14 ms, matrix = 80 × 80, FOV = 240 × 240 mm^2, number of slices = 20, slice thickness = 5 mm, gap = 0.5 mm, slice time (ST) = 36.25 ms, labeling time (LT) = 1650 ms, post-labeling delay (PLD) = 1525 ms, number of control/label pairs = 75, and scan duration = 10 min). For CBF quantification, a proton density image was acquired using the same sequence and positioning of ASL images, but with no labeling (TR/TE = 15,000/14 ms, matrix = 80 × 80, FOV = 240 × 240 mm^2, number of slices = 20, slice thickness = 5 mm, gap = 0.5 mm, number of repetitions = 5, and scan duration = 1 min and 30 s). In addition, for anatomical reference, a high-resolution 3D T1-weighted image was acquired (TR/TE = 7/3.1 ms, excitation angle = 8°, matrix = 240 × 240, FOV = 240 × 240 mm^2, number of slices = 160, slice thickness = 1 mm, and scan duration = 5 min and 30 s).

2.3. Image processing

Image processing was performed using SPM12 (http://www.fil.ion.

ucl.ac.uk/spm/), an open-source toolbox for ASL images (ASLtbx), and routines developed by our group in Matlab (TheMathWorks, Inc., USA). Statistical analyses were performed using R project for Statistical Computing (https://www.R-project.org). The processing pipeline was applied to each subject separately (Fig. 1). First, raw ASL images were head-motion corrected with a separate realignment for control and label images [14]. Image volumes in which the realignment caused a displacement of > 1 mm in any translational direction or > 1° in any rotational orientation were excluded. After the realignment, a coregistration with the anatomical reference was applied followed by the segmentation to obtain masks of gray matter (GM), white matter (WM) and cerebrospinal fluid (CSF).

Although the first step was a correction for head motion, residual motion effect may remain [26]. It mainly affects the CBF quantification since it is obtained by the subtraction between two images acquired at different times. So, to our purpose of studying functional connectivity, where fluctuations due to neuronal activity can be easily overwritten by noise, removing residual motion artifacts is relevant. Therefore, we evaluated the effect of removing residual motion artifacts and global signal fluctuations (RMAGSF) together, as proposed by Wang [20]: (1) all label and control images in the original acquisition order were input to the standard motion correction procedure and 3 translational and 3 rotational motion time courses were estimated for the entire ASL image series; (2) the zig-zagged label-control patterns were removed from those motion time courses through simple regressions; (3) cleaned motion parameters were used for denoising; (4) temporal filtering was done using a high-pass Butterworth filter (cut-off frequency = 0.04 Hz). Finally, a spatial smoothing with a Gaussian filter (FWHM = 4 mm) was performed.

The subtraction of control and label images was done to obtain perfusion-weighted maps using three different methods: simple, sinc and running [17] (Fig. 2). Then, CBF time series were calculated using a General Kinetic Model described by Buxton [13], considering the labeling efficiency 0.85, blood-brain water coefficient partition 0.9 g/ml, T_1 of tissue 1020 ms for GM and 770 ms for WM, and T_{1app} of blood 1650 ms.

All anatomical masks (GM, WM, CSF) and CBF time-series obtained with different filters and subtraction methods were normalized to MNI Space. Low-Pass temporal filtering (cut-off frequency = 0.07 Hz) was applied to limit the frequency band of signal analysis [27,28]. WM and CSF signals were removed through the COMPCOR algorithm [29], using a standard principal component analysis (PCA).

For all individual CBF data sets obtained from different subtraction methods, with and without RMAGSF removal process, temporal SNR (tSNR) was calculated by the ratio of the mean GM signal and its standard deviation. Statistical differences were analyzed with a two-way ANOVA test.

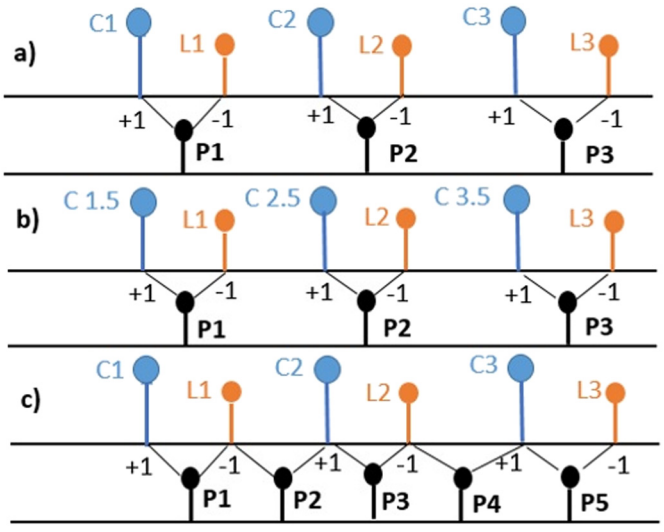

Fig. 2. Illustrative scheme of a) simple, b) sinc and c) running subtractions used to obtain the perfusion time series. C: control, L: label, P: perfusion.

2.4. Functional connectivity analysis

Functional connectivity (FC) was analyzed using CONN toolbox [30]. Group-level independent component analysis (ICA) was used to obtain the RBNs from CBF time series [31]. The number of independent components (ICs) was set to 20, and the dataset was analyzed with the fast-ICA algorithm [32] to extract the ICs. The individual temporal series and spatial maps were computed through the reverse reconstruction by the GICA1 algorithm [33]. RBNs were identified from the spatial correlation of the ICs with the CONN functional atlas and final visual verification. After identification, the number of significant correlations and anti-correlations ($p < 0.05$, FDR-corrected) were calculated for all RBNs.

Moreover, Pearson's correlation was calculated between the average time series of regions of interest (ROI), defined from 103 anatomical areas of the Harvard–Oxford atlas (excluding Vermis and Cerebellum areas not covered by our imaging acquisition). Six correlation matrices were obtained: two for each subtraction method, with and without RMAGSF removal. Then, three analyses were performed:

Analysis 1: To evaluate the effect of the subtraction method on FC, matrices obtained without RMAGSF removal were subtracted two by two (simple – sinc, running – sinc, and running - simple). The resulted matrices were thresholded using a one sample *t*-test ($p < 0.05$, FDR-corrected for multiple comparisons), followed by a binarization process to highlight differences in r-values that survived the test.

Analysis 2: To evaluate the effect of RMAGSF removal on FC, for each subtraction method, matrices obtained with and without RMAGSF removal were subtracted. The resulted matrices were thresholded using a one sample *t*-test ($p < 0.05$, FDR-corrected for multiple comparisons), followed by a binarization process to highlight differences in r-values that survived the test.

Analysis 3: For each subtraction method, matrices obtained with and without RMAGSF removal were thresholded using a one sample *t*-test ($p < 0.05$, FDR-corrected for multiple comparisons), followed by a binarization process to highlight significant correlation, and then subtracted to show the correlations that were significant for just one condition (with or without RMAGSF removal).

3. Results

Temporal SNR was obtained for all CBF time series. No statistically significant difference was observed among different subtraction methods; however, tSNR significantly increased after RMAGSF removal for simple and running subtraction ($p < 0.05$).

Our group-level ICA identified three RBNs regardless the subtraction method or RMAGSF removal: default mode (DMN), visual and sensory-motor (SMN) networks (Fig. 3). They all showed similar spatial correlation values with RBNs of the CONN functional atlas.

Compared to the networks obtained from sinc-subtracted images, simple subtraction resulted in networks with an increased number of correlated voxels (DMN – 14%, visual – 7%, SMN – 10%) and decreased number of anti-correlated voxels (DMN – 29%, visual – 26%, SMN – 9%). However, running-subtracted images resulted in networks with an increased number of both correlated (DMN – 38%, visual – 28%, SMN – 27%) and anti-correlated (DMN – 35%, visual – 38%, SMN – 34%) voxels.

The removal of RMAGSF also influenced the size of the networks. For the DMN, the filtering process decreased the number of correlated voxels (simple – 7%, sinc – 1%, running – 31%), but increased the number of anti-correlated voxels (simple – 22%, sinc – 19%, running – 7%). The decreases of correlated voxels were < 20% for both visual

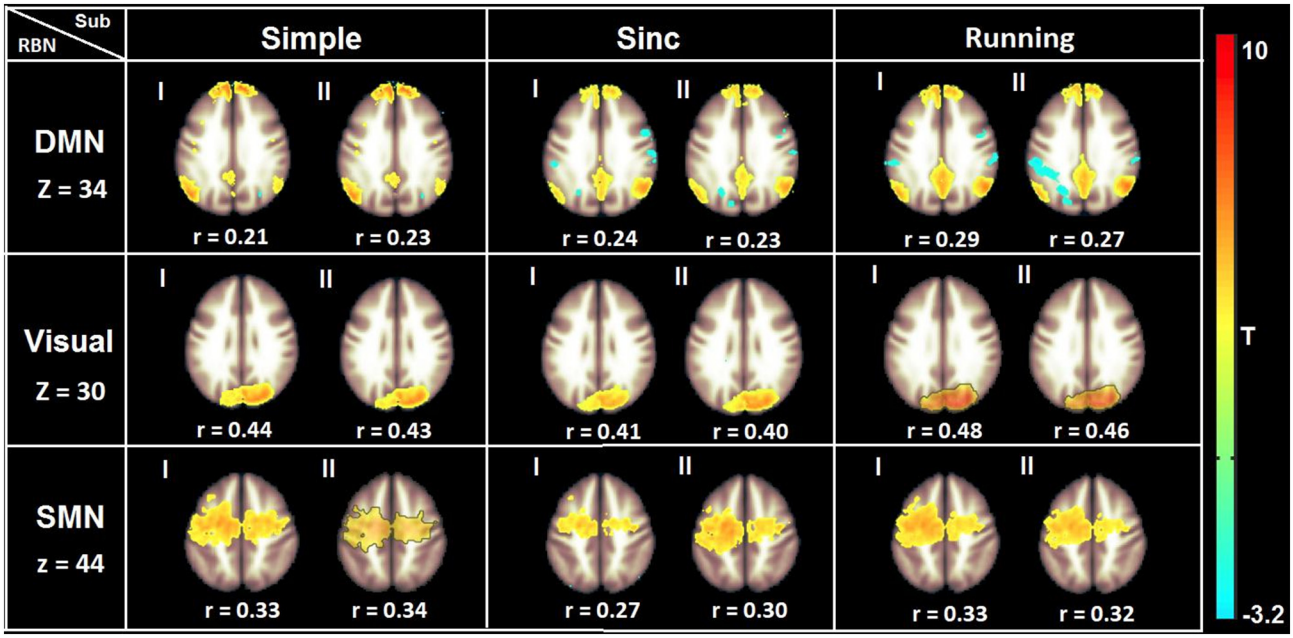

Fig. 3. Resting-state brain networks (default mode network – DMN, visual and sensory-motor – SMN) identified simple, sinc and running subtraction methods without (I) and with (II) removal of residual motion artifacts and global signal fluctuations (RMAGSF). R-values indicate the spatial correlation with Harvard–Oxford functional atlas.

network (simple – 18%, sinc – 9%, running – 5%) and SMN (simple – 4%, sinc – 3%, running – 7%). However, the increases of anti-correlated voxels were more accentuated (visual network: simple – 30%, sinc – 22%, running – 31%; SMN: simple – 20%, sinc – 14%, running – 29%).

Our ROI-to-ROI connectivity analysis showed that the subtraction method also influenced significantly the FC values (p-FDR < 0.05), especially the running subtraction. Approximately one-quarter of the ROI pairs showed a significant difference of r-values between the running subtraction and the other two methods (25%, for running – simple; 26%, for running – sinc) (Fig. 4).

We also evaluated the effect of RMAGSF removal on the FC values. Fig. 5 shows binarized matrices that highlight ROI pairs with statistically significant differences in r-values when comparing data obtained with and without RMAGSF removal (p-FDR < 0.05). Approximately one-quarter of the correlations significantly changed when using the RMAGSF removal for data obtained by sinc subtraction (24%) and one-third for running (33%) subtraction.

Moreover, Fig. 6 shows binarized matrices that highlight ROI pairs with statistically significant correlation only for data processed without (in blue) or with (in red) RMAGSF removal. If we only consider de number of significant correlations, the increase after RMAGSF removal was < 10% (simple – 2%, sinc – 0.2%, running – 10%), because the number of correlations that became significant after global signal regression was similar to the number that became not significant when applying it. However, as shown in Fig. 6, after RMAGSF removal, 8%, 31% and 32% of the correlations changed their status (significant or not) for simple, sinc and running subtraction, respectively.

4. Discussion

In the present study, we investigated the effects of subtraction methods and RMAGSF removal on tSNR values, identification of RBNs using ICA and ROI-based analysis of functional connectivity.

Regarding tSNR, higher values were observed after RMAGSF removal for CBF times series obtained with simple and running subtraction, as expected and previously reported [20,42]. However, RMAGSF removal did not affect the tSNR obtained with sinc subtraction, which may be related to the filtering role of sinc interpolation, which not only minimizes unrelated blood perfusion signals but also improves image quality [14,19]. Moreover, our results showed that the use of running subtraction does not provide significant higher tSNR compared to simple subtraction as occurred in previous studies [10,20].

Regardless the subtraction method or filtering choice, default mode, visual and sensory-motor networks were identified by ICA with similar spatial correlation to the functional templates. These networks are the ones that appear mostly in the literature, due to individual behavior in resting state, with eyes open, related to mind-wandering, visual cortex activity and movements due to fatigue during the image acquisition [34]. However, other common RBNs were not obtained, such as the left and right executive control networks previously shown using pCASL with 3D background suppressed GRASE readout [10]. One possible explanation is related to the 2D pCASL images that usually show intrinsic low SNR, spatial resolution, and sensitivity to CBF value differentiation in a voxel level [35]. These characteristics may affect ICA results, which is performed voxel-wisely and is very sensitive to spatial-temporal conditions of the acquired image. Moreover, many tools used for RBN identification, such as the mathematical processes involved with group ICA, group-level back reconstruction algorithm and number of ICs can act directly in the final results [36].

Regarding the number of correlated and anti-correlated voxels, we observed that there was an increase in anti-correlations when the removal of RMAGSF was applied, as commented in a previous study [23], especially for the running subtraction. However, due to many aspects, some researchers have discussed that global signal regression may show a two-sided influence. While some reported a specificity of positive correlations with an improvement in anatomical connectivity correspondence [37], another speculated a potentially spurious “artefactual” correlation in the modeled data [38]. Then, all these factors influence FC results and should be considered in the analysis [39].

In an ROI-to-ROI level, running subtraction seems to introduce more correlations in the results. The correlation matrix obtained by running subtraction, when compared to other methods, showed more changes after RMAGSF use, which suggests more presence of potential noise that can interfere with FC analysis. One possible reason that can explain this result is related to the increase in CBF time series length. By definition, Pearson's correlation is directly influenced by sample characteristics as

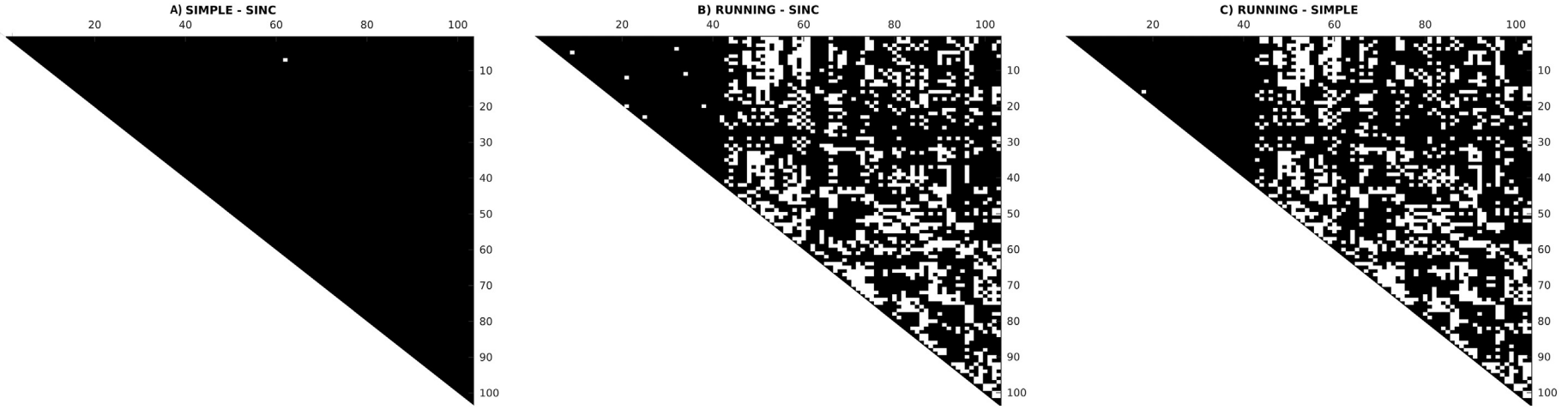

Fig. 4. Binarized matrices that highlight (in white) ROI pairs with statistically significant differences in r-values ($p < 0.05$, FDR-corrected for multiple comparisons) when comparing data obtained with different subtraction methods, without RMAGSF removal, two by two: A) simple – sinc, B) running – sinc, and C) running - simple). These are the results of *Analysis 1*, Section 2.4.

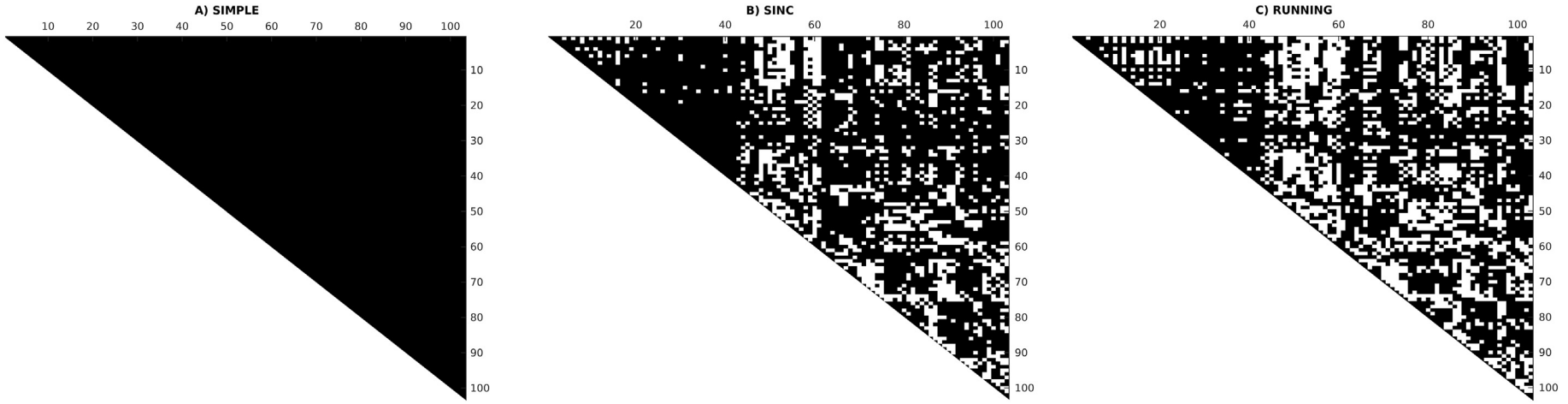

Fig. 5. Binarized matrices that highlight (in white) ROI pairs with statistically significant differences in r-values ($p < 0.05$, FDR-corrected for multiple comparisons) when comparing data obtained with and without RMAGSF removal, for each subtraction method: A) simple, B) sinc, and C) running. These are the results of *Analysis 2*, Section 2.4.

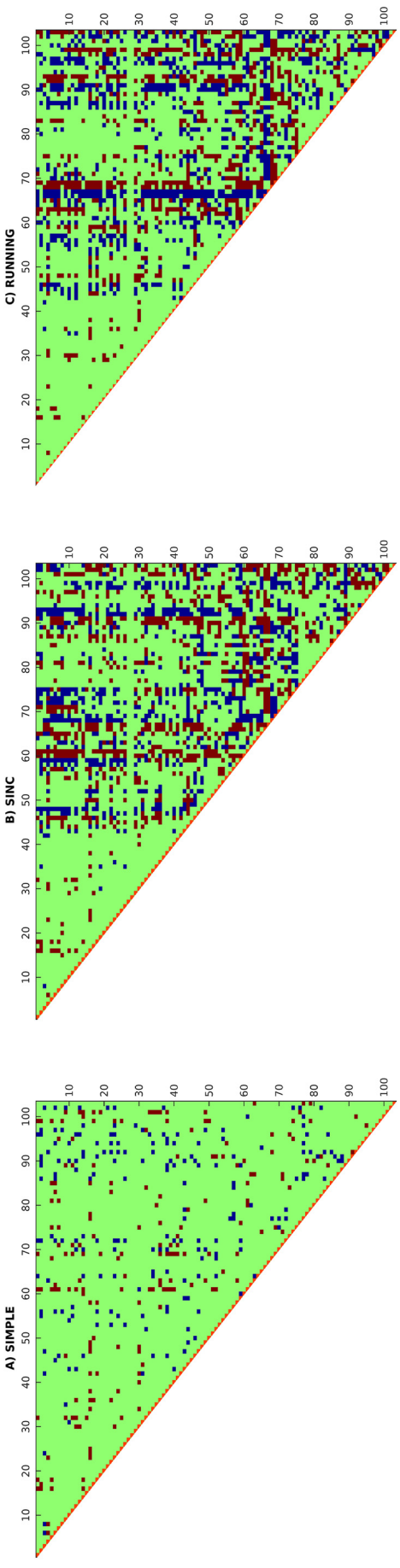

Fig. 6. Binarized matrices that highlight correlations statistically significant only for data without (in blue) or with (in red) RMAGSF removal ($p < 0.05$, FDR-corrected for multiple comparisons), for each subtraction method: A) simple, B) sinc and C) running. These are the results of *Analysis 3*, Section 2.4. (For interpretation of the references to colour in this figure legend, the reader is referred to the web version of this article.)

standard deviation and covariance between two datasets [40]. In the context of functional ASL analysis, the increase of CBF time points not only changes the CBF time evolution pattern but also can change its statistical parameters and directly impact its properties like statistical significance and FC calculation. Beyond that, the use of running subtraction may result in bigger contamination of other signals and effects that are not necessarily related to blood perfusion, like BOLD contamination [10,41].

Our results also showed that there is a difference in connectivity pattern since there are new significant correlations and loss of others after the RMAGSF removal. For all analysis performed considering the results obtained by three subtraction methods, the number of significant correlations always increased, but not in the same proportion. Running subtraction was the method that suffered more with the introduction of correlations and changes in their statistical values. In contrast, r-values of data obtained with simple subtraction seemed to be less affected by RMAGSF removal. In addition, although the absolute number of significant correlations increased < 10% after RMAGSF removal, up to 32% of the correlations changed their status of significance, which might interfere with data interpretation.

It is important to note that the above ROI-based results may be affected by the r-value thresholding. Here we used a *p*-value approach considering the FDR-correction for multiple comparisons which may lead to different results when comparing to other studies on FC analysis. Moreover, in more heterogeneous groups, such as elderly or patients, the result of RMAGSF removal could be even more accentuated due to their physiological conditions and head movement during the exam [39].

5. Conclusion

This study evaluated the effects of different subtractions and RMAGSF removal on the identification of RBNs and functional connectivity analysis. Our results showed no significant impact on network identification, but the RMAGSF removal increased the anti-correlations for all approaches. For the ROI-based analysis, the results were significantly influenced by the subtraction method and RMAGSF removal, especially for the running subtraction. Therefore, taking our results and the whole discussion together, we understand that for an exploratory assessment of the brain, one could avoid removing RMAGSF to not bias FC measures, but could use sinc subtraction to minimize low-frequency contamination. However, CBF signal specificity, frequency range for filtering purposes, and effects on different subject groups still need to be assessed in future studies.

Conflicts of interest

The authors declare that they have no conflict of interest.

Funding

This work was supported by the CAPES (Coordination for the Improvement of Higher Education Personnel).

References

[1] Liang X, Connelly A, Calamante F. Graph analysis of resting-state ASL perfusion MRI data: nonlinear correlations among CBF and network metrics. Neuroimage 2014;87:265–75. http://dx.doi.org/10.1016/j.neuroimage.2013.11.013.

[2] Jann K, Gee DG, Kilroy E, Schwab S, Smith RX, Cannon TD, et al. Functional connectivity in BOLD and CBF data: SIMILARITY and reliability of resting brain networks. Neuroimage 2015;106:111–22. http://dx.doi.org/10.1016/j.neuroimage.2014.11.028.

[3] Mayhew SD, Mullinger KJ, Bagshaw AP, Bowtell R, Francis ST. Investigating intrinsic connectivity networks using simultaneous BOLD and CBF measurements. Neuroimage 2014;99:111–21. http://dx.doi.org/10.1016/j.neuroimage.2014.05.042.

[4] Andreotti J, Jann K, Melie-Garcia L, Giezendanner S, Dierks T, Federspiel A.

Repeatability analysis of global and local metrics of brain structural networks. Brain Connect 2014;4:203–20. http://dx.doi.org/10.1089/brain.2013.0202.
[5] Warnock G, Özbay PS, Kuhn FP, Nanz D, Buck A, Boss A, et al. Reduction of BOLD interference in pseudo-continuous arterial spin labeling: towards quantitative fMRI. J Cereb Blood Flow Metab 2017:1–10. http://dx.doi.org/10.1177/0271678X17704785.
[6] Detre JA, Wang J. Technical aspects and utility of fMRI using BOLD and ASL. Clin Neurophysiol 2002;113:621–34. http://dx.doi.org/10.1016/S1388-2457(02)00038-X.
[7] Chuang KH, van Gelderen P, Merkle H, Bodurka J, Ikonomidou VN, Koretsky AP, et al. Mapping resting-state functional connectivity using perfusion MRI. Neuroimage 2008;40:1595–605. http://dx.doi.org/10.1016/j.neuroimage.2008.01.006.
[8] Steketee RME, Mutsaerts HJMM, Bron EE, Van Osch MJP, Majoie CBLM, Van Der Lugt A, et al. Quantitative functional arterial spin labeling (fASL) MRI - sensitivity and reproducibility of regional CBF changes using pseudo-continuous ASL product sequences. PLoS One 2015;10:1–17. http://dx.doi.org/10.1371/journal.pone.0132929.
[9] Zhu S, Fang Z, Hu S, Wang Z, Rao H. Resting state brain function analysis using concurrent BOLD in ASL perfusion fMRI. PLoS One 2013;8:4–13. http://dx.doi.org/10.1371/journal.pone.0065884.
[10] Chen J, Jann K, Wang DJ. Characterizing resting-state brain function using arterial-spin labeling. Brain Connect 2015;5:527–42. http://dx.doi.org/10.1089/brain.2015.0344.
[11] Liu TT, Wong EC. A signal processing model for arterial spin labeling functional MRI. Neuroimage 2005;24:207–15. http://dx.doi.org/10.1016/j.neuroimage.2004.09.047.
[12] Buxton RB, Frank LR, Wong EC, Siewert B, Warach S, Edelman RR. A general kinetic model for quantitative perfusion imaging with arterial spin labeling. Magn Reson Med 1998;40:383–96. http://dx.doi.org/10.1002/mrm.1910400308.
[13] Buxton RB. Quantifying CBF with arterial spin labeling. J Magn Reson Imaging 2005;22(6):723. http://dx.doi.org/10.1002/jmri.20462.
[14] Wang Z, Aguirre GK, Rao H, Wang J, Fernández-Seara MA, Childress AR, et al. Empirical optimization of ASL data analysis using an ASL data processing toolbox: ASLtbx. Magn Reson Imaging 2008;26:261–9. http://dx.doi.org/10.1016/j.mri.2007.07.003.
[15] Aguirre GK, Detre JA, Zarahn E, Alsop DC. Experimental design and the relative sensitivity of BOLD and perfusion fMRI. Neuroimage 2002;15:488–500. http://dx.doi.org/10.1006/nimg.2001.0990.
[16] Lu H, Donahue MJ, Van Zijl PCM. Detrimental effects of BOLD signal in arterial spin labeling fMRI at high field strength. Magn Reson Med 2006;56:546–52. http://dx.doi.org/10.1002/mrm.20976.
[17] Alsop DC, Detre JA, Golay X, Gunther M, Hendrikse J, Hernandez-Garcia L, et al. Recommended implementation of arterial spin-labeled perfusion mri for clinical applications: a consensus of the ISMRM perfusion study group and the European consortium for ASL in dementia. Magn Reson Med 2015;73:102–16. http://dx.doi.org/10.1002/mrm.25197.
[18] Jahanian H, Peltier S, Noll DC, Garcia LH. Arterial cerebral blood volume-weighted functional MRI using pseudocontinuous arterial spin tagging (AVAST). Magn Reson Med 2015;73:1053–64. http://dx.doi.org/10.1002/mrm.25220.
[19] Aguirre GK, Detre JA. Experimental design and the relative sensitivity of BOLD and Perfusion fMRI. 15. 2002. p. 488–500. http://dx.doi.org/10.1006/nimg.2001.0990.
[20] Wang Z. Improving cerebral blood flow quantification for arterial spin labeled perfusion MRI by removing residual motion artifacts and global signal fluctuations. Magn Reson Imaging 2012;30:1409–15. http://dx.doi.org/10.1016/j.mri.2012.05.004.
[21] Dai W, Varma G, Scheidegger R, Alsop DC. Quantifying fluctuations of resting state networks using arterial spin labeling perfusion MRI. J Cereb Blood Flow Metab 2015;36:463–73. http://dx.doi.org/10.1177/0271678X15615339.
[22] Aguirre GK, Zarahn E, D'Esposito M. Empirical analyses of BOLD fMRI statistics. Neuroimage 1997;5:199–212. http://dx.doi.org/10.1006/nimg.1997.0264.
[23] Murphy K, Birn RM, Handwerker DA, Jones TB, Bandettini PA. The impact of global signal regression on resting state correlations: are anti-correlated networks introduced? Neuroimage 2009;44:893–905. http://dx.doi.org/10.1016/j.neuroimage.2008.09.036.
[24] Bright MG, Murphy K. Is fMRI "noise" really noise? Resting state nuisance regressors remove variance with network structure. Neuroimage 2015;114:158–69. http://dx.doi.org/10.1016/j.neuroimage.2015.03.070.
[25] Leopold DA, Maier A. Ongoing physiological processes in the cerebral cortex. Neuroimage 2012;62:2190–200. http://dx.doi.org/10.1016/j.neuroimage.2011.10.059.
[26] Friston KJ, Williams S, Howard R, Frackowiak RSJ, Turner R. Movement-related effects in fMRI time-series. Magn Reson Med 1996;35:346–55. http://dx.doi.org/10.1002/mrm.1910350312.
[27] Mengual E, Vidorreta M, Castellanos G, Irigoyen J, Erro E. Resting state functional connectivity of the subthalamic nucleus in Parkinson's disease assessed using arterial spin-labeled perfusion fMRI. Hum Brain Mapp 2015;36:1937–50. http://dx.doi.org/10.1002/hbm.22747.
[28] Boissoneault J, Letzen J, Lai S, O'Shea A, Craggs J, Robinson ME, et al. Abnormal resting state functional connectivity in patients with chronic fatigue syndrome: an arterial spin-labeling fMRI study. Magn Reson Imaging 2016;34:603–8. http://dx.doi.org/10.1016/j.mri.2015.12.008.
[29] Behzadi Y, Restom K, Liau J, Liu TT. A component based noise correction method (CompCor) for BOLD and perfusion based fMRI. Neuroimage 2007;37:90–101. http://dx.doi.org/10.1016/j.neuroimage.2007.04.042.
[30] Whitfield-Gabrieli S, Nieto-Castanon A. *Conn*: a functional connectivity toolbox for correlated and Anticorrelated brain networks. Brain Connect 2012;2:125–41. http://dx.doi.org/10.1089/brain.2012.0073.
[31] Beckmann CF, DeLuca M, Devlin JT, Smith SM. Investigations into resting-state connectivity using independent component analysis. Philos Trans R Soc B Biol Sci 2005;360:1001–13. http://dx.doi.org/10.1098/rstb.2005.1634.
[32] Hyvärinen A, Oja E. A fast fixed-point algorithm for independent component analysis. Neural Comput 1997;9:1483–92. http://dx.doi.org/10.1162/neco.1997.9.7.1483.
[33] Calhoun VD, Adali T, Pearlson GD, Pekar JJ. A method for making group inferences from functional MRI data using independent component analysis. Hum Brain Mapp 2001;14:140–51. http://dx.doi.org/10.1002/hbm.
[34] Zou Q, Yuan BK, Gu H, Liu D, Wang DJJ, Gao JH, et al. Detecting static and dynamic differences between eyes-closed and eyes-open resting states using ASL and BOLD fMRI. PLoS One 2015;10:1–12. http://dx.doi.org/10.1371/journal.pone.0121757.
[35] Borogovac A, Asllani I. Arterial spin labeling (ASL) fMRI: advantages, theoretical constrains and experimental challenges in neurosciences. Int J Biomed Imaging 2012;2012:1–13. http://dx.doi.org/10.1155/2012/818456.
[36] Cole DM, Smith SM, Beckmann CF. Advances and pitfalls in the analysis and interpretation of resting-state FMRI data. Front Syst Neurosci 2010;4:1–15. http://dx.doi.org/10.3389/fnsys.2010.00008.
[37] Fox M, Zhang D. The global signal and observed anticorrelated resting state brain networks. J Neurophysiol 2009;101:3270–83. http://dx.doi.org/10.1152/jn.90777.2008.
[38] Anderson JS, Druzgal TJ, Lopez-Larson M, Jeong EK, Krishnaji D, Yurgelun-Todd D. Network anticorrelations, global regression, and phase-shifted soft tissue correction (PSTCor). Hum Brain Mapp 2011;32:919–34. http://dx.doi.org/10.1002/hbm.21079.Network.
[39] Murphy K, Fox MD. Towards a consensus regarding global signal regression for resting state functional connectivity MRI. Neuroimage 2017;154:169–73. http://dx.doi.org/10.1016/j.neuroimage.2016.11.052.
[40] Lee MH, Smyser CD, Shimony JS. Resting-state fMRI: a review of methods and clinical applications. Am J Neuroradiol 2013;34:1866–72. http://dx.doi.org/10.3174/ajnr.A3263.
[41] Rogers BP, Morgan VL, Newton AT, Gore JC. Assessing functional connectivity in the human brain by fMRI. Magn Reson Imaging 2007;25:1347–57. http://dx.doi.org/10.1016/j.mri.2007.03.007.
[42] Jann K, Smith RX, Piedra EAR, Dapretto M, Wang DJJ. Noise reduction in arterial spin labeling based functional connectivity using nuisance variables. Front Neurosci 2016;10:1–13. http://dx.doi.org/10.3389/fnins.2016.00371.